PCCP

Use of Bound State Methods to Calculate Partial and Total Widths of Shape Resonances

Journal:	*Physical Chemistry Chemical Physics*
Manuscript ID	CP-ART-08-2023-004154.R1
Article Type:	Paper
Date Submitted by the Author:	23-Oct-2023

Complete List of Authors:	Jordan, Kenneth; University of Pittsburgh, Department of Chemistry Falcetta, Michael; Grove City College Fair, Mark; Grove City College Slimak, Stephen; University of Pittsburgh, Department of Chemistry Sommerfeld, Thomas; Southeastern Louisiana University, Department of Chemistry and Physics

Use of Bound State Methods to Calculate Partial and Total Widths of Shape Resonances

Michael F. Falcetta,*[a] Mark C. Fair,[b] Stephen R. Slimak,[c] Kenneth D. Jordan,*[c] and Thomas Sommerfeld*[d]
[a] Department of Chemistry, Grove City College, Grove City, PA 16127, USA
[b] Departments of Mechanical Engineering and Physics, Grove City College, Grove City, PA 16127, USA
[c] Department of Chemistry, University of Pittsburgh, Pittsburgh, PA 15260, USA
[d] Department of Chemistry, Southeastern Louisiana University, Hammond, LA 70402, USA

Abstract: In this work we study the $^2\Pi$ resonances of a two-site model system designed to mimic a smooth transition from the $^2\Pi_g$ temporary anion of N_2 to the $^2\Pi$ temporary anion of CO. The model system possesses the advantage that scattering and bound state (L^2) methods can be directly compared without obfuscating electron-correlation effects. Specifically, we compare resonance parameters obtained with the complex Kohn variational (CKV) method with those from stabilization, complex absorbing potential, and regularized analytical continuation calculations. The CKV calculations provide *p*-wave and *d*-wave widths, the sum of which provides a good approximation of the total width. Then we demonstrate that the width obtained with modified bound state methods depends on the basis set employed: It can be the total width, a partial width, or an ill-defined sum of partial widths. Provided the basis set is chosen appropriately, widths from bound state methods agree well with the CKV results.

1 Introduction

Anion states lying energetically above the ground state of the neutral molecule can be probed experimentally by electron scattering[1-4] or, in the case of systems with a bound ground state anion, by photodetachment spectroscopy.[5] Such anion states, termed temporary anions (TAs), are subject to decay by electron detachment. Despite lifetimes typically as short as a few fs, temporary anions play an important role in a wide range of processes including electron-induced DNA damage[6-8] and the operation of certain laser systems.[9] As such there is considerable interest in developing robust computational methodologies to model electron capture and detachment.[10-34]

A TA can be characterized by a complex resonance energy E_{Res},

$$E_{Res} = E_r - i\Gamma/2 \quad (1)$$

where E_r is the real part of the resonance energy relative to the neutral molecule and Γ, the resonance width, is inversely related to the anion lifetime.[35] There are various types of TAs.[1-3] Here our focus is on TAs that result from electron capture into empty valence orbitals of closed-shell neutral molecules. Such TA states often dominate low-energy electron-molecule scattering cross sections and are termed shape resonances, emphasizing the fact that the finite lifetime is due to the shape of the potential that derives from the combination of short-range forces and angular momentum contributions.[1-3,36] In the case of non-zero angular momentum, this leads to a barrier through which the electron must tunnel in the attachment and detachment processes. The charge distribution of the orbital involved in the electron capture is crucial in determining the angular distribution of resonant electron scattering.

As noted above, several computational methods have been introduced for characterizing temporary anions and other resonances. One class of methods including the complex Kohn variational (CKV) method and the R-Matrix methods[10-12] is based on scattering theory and provides quantities such as the

T-matrix and eigenphase sum. These quantities lead directly to cross sections and can be used to calculate resonance energy and width.

Accurate characterization of resonances of polyatomic molecules with scattering methods, however, is computationally very demanding due to the role of electron correlation. State-of-the-art scattering calculations tend to use configuration interaction treatments which make it hard to treat electron correlation effects in the ground state neutral and the anionic states in a balanced manner. Bound state methods have the advantage of being able to use high-level electronic structure algorithms to treat the anion as well as neutral systems, particularly methods that are size consistent and size-extensive, thus allowing for a balanced treatment of electron correlation in the neutral and anionic states. For this reason, many computational studies of temporary anions of polyatomic molecules have employed modified bound state methods employing L^2 wave functions. These include the stabilization method,[15-21] regularized analytic continuation (RAC),[22-24] and the complex absorbing potential (CAP) method.[25-30] Details of the CKV, stabilization, RAC, and CAP methods will be given below.

For the well-studied $^2\Pi_g$ valence anion of N_2, bound state[16,17,20,29,32-34] and scattering calculations carried out with high level treatment of electron correlation[14] have been found to give similar resonance parameters. Yet, as will be discussed below, this is not necessarily the case for the resonance widths for heteronuclear diatomic molecules or large organic molecules such as anthracene for which multiple partial waves contribute to the various TA resonances.[37]

In this work we consider a one-electron model system for which we can vary the asymmetry of the potential and for which we can apply both scattering and bound state methods of treating a resonance, facilitating comparison of resonance parameters obtained from the two approaches. In addition, use of a one-electron model eliminates effects of electron correlation on the resonance parameters and allows the use of highly flexible one-particle basis sets. The model potentials will be used in calculations extracting both partial (angular momentum dependent) and total widths using the various approaches. The direct comparison of three bound state methods and a scattering-based approach on the same non-spherical potential, with basis sets that give well-converged results, is a distinctive contribution to the field.

For spherical target systems the scattering problem is naturally treated in terms of partial waves, for which the electron orbital angular momentum, characterized by the quantum number l, is a good quantum number. However, for molecules l is not a good quantum number and more than one value of l contributes to the resonant scattering process. For small highly symmetric molecules the lowest, symmetry-allowed value of l (l = 2 in the case of the $^2\Pi_g$ valence anion of N_2) dominates the scattering via the lowest energy shape resonance. However, in general two or more partial waves are important, with the shape of the orbital involved in electron capture being a major factor in determining the partial widths. For example, for the $^2\Pi$ shape resonance of CO^- inclusion of both *p* and *d* partial waves is necessary for accurate calculation of the differential scattering cross section and vibrational excitation cross sections in the energy region of resonance.[18,38-42] This can be seen qualitatively from examination of the shape of the lowest energy valence π^* orbital of neutral CO: Because this orbital has different contributions of the *p* orbitals on the two atomic sites, it has sizable l = 1 and 2 components. In polyatomic molecules, such as anthracene, even though the overall symmetry is high, there can be

strong admixture of several l values in partial wave expansions of the low-lying π^* orbitals.[37] Moreover, in a many-electron system, electron correlation effects impact the relative importance of the various partial waves.

In resonances where two or more partial waves are important, prediction of the angular distribution of the scattered electrons requires a weighted contribution from the relevant partial waves. Chang presented a methodology, based on frame transformation theory, that determines angular distributions without the assumption that l is a good quantum number.[40,41] Implementation of Chang's approach requires l-dependent probabilities for electron capture (and detachment) that are of the form $\sqrt{\frac{\Gamma_l}{2\pi}}$, where Γ_l is the partial width associated with the l^{th} partial wave. For narrow resonances, the individual partial widths sum to Γ, the total width in eqn (1).[43] Although it is usually assumed that the leading partial wave has the greatest partial width, this is not necessarily the case as shown in Ref. 18.

Surprisingly, in most studies of TAs using bound state methods the nature of the widths obtained has not been addressed. We note that Bentley and Chipman considered complexities associated with extracting widths from stabilization calculations for a resonance that can decay into different states.[44] Specifically, they showed that depending on how the calculations were carried out, the widths obtained were neither partial nor total. Moreover, we have found in applying the stabilization method as normally employed to polyatomic molecules very different widths result depending on the range of data used, suggesting that the calculations may not give accurate total widths in all cases, but rather some combination of partial widths with improper weighting. This suggests that the issue raised by Bentley and Chipman is present in systems in which different partial waves are important in electron capture and detachment.

Stabilization calculations as usually carried out on molecules employ diffuse atomic basis functions of the appropriate symmetry on all relevant atoms. In the 2016 study of the $^2\Pi$ resonance of CO^- in Ref. 18 it was demonstrated that by employing instead single center expansions of diffuse *p* or diffuse *d* functions in the one particle basis set used in the calculations, separate *p*-wave and *d*-wave widths could be obtained.

To further investigate the issues raised above, we consider a model potential consisting of two spherical Gaussian wells. When the wells are identical, the system serves as a model for the $^2\Pi_g$ TA state of N_2 for which the resonance is well characterized as *d*-wave. By making the two wells nonequivalent, both *p*-wave and *d*-wave character become important, similar to the $^2\Pi$ TA state of CO. The model system employed permits tuning the degree of asymmetry and, hence, the relative importance of *p*- and *d*-wave components. As a result, it is relevant for describing changes that could occur upon geometric distortion or describing the impact of mixing of partial waves in an unfilled orbital in a polyatomic molecule. The lowest energy resonance of this model potential is characterized using the CKV, stabilization, CAP, and RAC methods.

The goals of the current study are (1) to investigate whether the approach used previously in conjunction with the stabilization method to obtain partial widths of the $^2\Pi$ TA state of CO[18] also works with other bound state methods, such as CAP and RAC, (2) to explore whether the partial widths obtained from bound state methods agree with those from scattering calculations, and (3) to analyze the sensitivity of the widths from stabilization calculations to the choice of basis set.

2 Methodology

To examine the nature of the resonance widths obtained from various theoretical methods we employ a one-electron system with two attractive Gaussian wells. Site 1 is located at (0, 0, 1) bohr, and site 2 is located at (0, 0, -1) bohr with position vectors $\boldsymbol{r_1}$ and $\boldsymbol{r_2}$, respectively. The potential has the form

$$V = V_{01}e^{-\beta_1|\boldsymbol{r}-\boldsymbol{r_1}|^2} + V_{02}e^{-\beta_2|\boldsymbol{r}-\boldsymbol{r_2}|^2} \quad (2)$$

V_{01} is fixed at -36.135 hartrees (E_h) and β_1 is fixed at -6.0 $bohr^{-2}$. The parameters for site 2 are systematically varied, taking the values in Table 1.

TABLE 1. Parameter sets for site 2 in the model potential defined by equation 2.

Set	V_{02} (E_h)	β_2 ($bohr^{-2}$)
A	-36.13500	6.000
B	-36.13995	5.960
C	-36.14490	5.920
D	-36.14985	5.880
E	-36.15480	5.875
F	-36.15975	5.850

Set A corresponds to a symmetric double well potential, while sets B through F are increasingly more asymmetric double well potentials. Only states of Π symmetry are considered. With the given parameters, the potential supports one bound state of Π symmetry and a low-lying Π shape resonance which is the focus of this study. The system is treated with four different theoretical methods described below.

2.1 Complex Kohn variational method

We consider resonance parameters obtained from the CKV method[10,12] to be most definitive as this method explicitly considers the continuum, thus avoiding the need for additional steps, e.g., analytic continuation or modifying the potential, required in the bound state methods to obtain the complex resonance energy. For the CKV calculations the outgoing trial wave function is

$$\psi^{trial}_{l_{out}m_{out}} = \sum_{l_{in}} \frac{[f_{l_{in}}(r)\delta_{l_{in}l_{out}} + T_{l_{in}l_{out}}g_{l_{in}}(r)]Y_{l_{out}m_{out}}(\hat{r})}{r} + \sum_{k,i} c_{k,i}\varphi_{k,i}(\boldsymbol{r_i}) \quad (3)$$

where the $Y_{lm}(\hat{r})$ are real spherical harmonics, the $\varphi_{k,i}(r_i)$ are Gaussian type basis functions centered at site *i*, and $\boldsymbol{r_i}$ is the position vector relative to the origin. f_l and g_l, are the regular and outgoing Ricatti-Bessel functions, respectively. The wave function in the region where the potential is nonnegligible is described by 15 even-tempered Gaussian *p* functions starting at exponent 700, decreasing by a factor of 2.5, and centered at both $\boldsymbol{r_1}$ and $\boldsymbol{r_2}$. For the model potentials of interest, well converged results are obtained using only l values of 1, 2, and 3 and *m* was restricted to 1, consistent with Π symmetry. The $T_{l_{in}l_{out}}$matrix elements in eqn (3), found as variational parameters in the CKV calculation, can be used to calculate differential and integral cross sections. The inclusion of the subscripts on quantum numbers indicating electron capture (*in*) or detachment (*out*) are used here to emphasize a simple physical picture, in lieu of the more traditional l and l'. In the context of the frame transformation approach of

Chang[40,41], matrix elements for which $l_{in} \neq l_{out}$ imply a change in the orbital angular momentum of the electron during the scattering event. In real, molecular situations the total angular momentum is conserved by a concomitant change in the rotational angular momentum, with the small change in the magnitude of the momentum of the scattered electron being ignored because it is not resolvable in typical experiments. Additional details of the CKV method can be found in reference 12.

The extraction of the resonance parameters from the CKV data proceeds via Breit-Wigner approximation. Taylor[45] showed that the Breit-Wigner approximation applied to a resonance formed by capture of the l_{in} partial wave and decaying via the l_{out} partial wave (assuming the magnitude of the entrance and exit momentum of the electron is the same) leads to the following form for the absolute square of the scattering amplitude, $|f_{l_{in},l_{out}}|^2$

$$|f_{l_{in},l_{out}}|^2 = \frac{\left(\frac{\Gamma_{l_{in}}}{2}\right)\left(\frac{\Gamma_{l_{out}}}{2}\right)}{k^2\left((E-E_r)^2+\frac{\Gamma^2}{4}\right)}, \quad (4)$$

where $\Gamma_{l_{in}}$ is the partial width for l_{in}, governing the probability an electron with that orbital angular momentum being captured and $\Gamma_{l_{out}}$ is the analogous partial width for electron detachment. The total width, Γ, in the present work is taken as the sum of the sum of the partial widths, which is rigorously true only for narrow resonances. In the present work l_{in} and l_{out} are limited to being either one or two, since for the potentials of interest T_{33}, T_{23} and T_{13} are negligible over the range of energies considered.

Since $|T_{l_{in},l_{out}}|^2 = k^2|f_{l_{in},l_{out}}|^2$,

$$|T_{l_{in},l_{out}}|^2 = \frac{\left(\frac{\Gamma_{l_{in}}}{2}\right)\left(\frac{\Gamma_{l_{out}}}{2}\right)}{\left((E-E_r)^2+\Gamma^2/4\right)} \quad (5)$$

Thus, at each energy $|T_{11}|^2$, $|T_{12}|^2$, and $|T_{22}|^2$ can be expressed as a function of the resonance energy and partial widths, assuming validity of the Breit-Wigner expression.

As demonstrated by Fano[46] as well as Blatt and Weisskopf[47], the interaction of a discrete state with two autoionization continua can alter the shape of peaks arising from such states in spectra and scattering cross sections when the entrance and exit channels are identical. We find that the application of this approach adequately accounts for the pronounced asymmetry in the peak shape of the $|T_{11}|^2$ vs E curve shown in Fig. 1, as well as the lesser asymmetry in the shape of the $|T_{22}|^2$ vs E curve. Following equation VIII.7.20 of Ref. 47 an l-dependent parameter, $\delta_{bg,l}$, is added for the case of $l_{in} = l_{out}$ which controls the asymmetry. Noting that $\Gamma_{l_{in}} = \Gamma_{l_{out}} = \Gamma_l$, eqn (5) can be modified for $|T_{11}|^2$ and $|T_{22}|$ as follows:

$$|T_{l,l}|^2 = \left|\frac{i\frac{\Gamma_l}{2}}{E-E_r+i\Gamma/2} + \frac{e^{-2i\delta_{bg,l}}-1}{2}\right|^2 \quad (6)$$

For each set of potential parameters, the CKV data for the absolute squares of all three energy-dependent T-matrix elements are simultaneously least squares fit ($|T_{12}|^2$ to the functional form given by eqn (5) and $|T_{11}|^2$ and $|T_{22}|^2$ to that of eqn (6)) and values for E_r, Γ_1, Γ_2, $\delta_{bg,1}$, $\delta_{bg,2}$ are obtained, allowing direct comparison with the complex resonance energies obtained from the bound state methods. The

range of energy values considered in the fit are limited to $E_r - 4\Gamma$ to $E_r + 4\Gamma$. Using an expanded range from $E_r - 6\Gamma$ to $E_r + 6\Gamma$ has negligible impact on the resonance parameters. For set A, which has no *p*-wave contribution, only the $|T_{22}|^2$ vs *E* curve was fit, with the assumption that $\Gamma_1 = 0$.

Fig. 1 shows $|T_{pp}|^2$, $|T_{dd}|^2$, and $|T_{pd}|^2$ as a function of energy for potential parameter set C, where l = 1 and 2 have been replaced by *p* and by *d*, respectively. All three quantities display a pronounced peak near E_r = 2.50 eV, due to the resonance. The fits, shown as solid lines, are in excellent agreement with the CKV results. The asymmetry in the $|T_{pp}|^2$ and $|T_{dd}|^2$ curves is accounted for by the background term in eqn (6), as are the small difference in the peak positions in each of the curves.

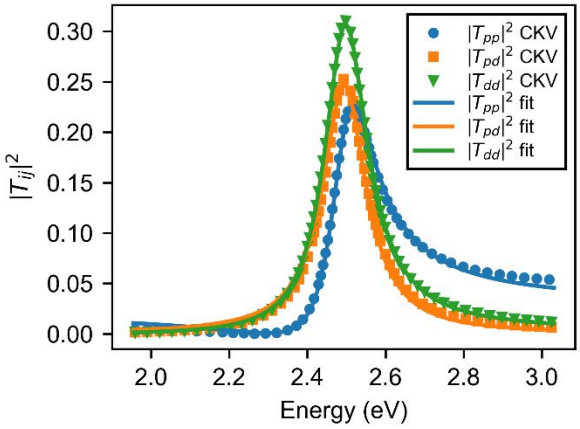

Fig. 1 $|T_{pp}|^2$ (blue dots), $|T_{pd}|^2$ (orange squares), and $|T_{dd}|^2$ (green triangles) obtained from CKV calculations for potential set C as a function of energy (eV). Also shown are the fits obtained with equations (5) and (6) for $|T_{pp}|^2$ (blue line), $|T_{pd}|^2$ (orange line), and $|T_{dd}|^2$ (green line).

2.2 Bound state methods

Straightforward application of standard quantum chemistry methods to TAs is not possible when using flexible basis sets due to the presence of discretized continuum (DC) solutions that fall energetically below and in the same energy range as the temporary anion of interest. The DC solutions correspond to a free electron as described by the finite basis set. Thus, with flexible basis sets, standard bound state methods will collapse onto a DC level. The stabilization, CAP, and RAC methods are all designed to avoid this problem.

The variant of the stabilization method employed here has been described in detail previously and involves the calculation of the energies of multiple eigenvalues of the appropriate symmetry of the excess electron system as a function of a scale parameter, *z*, that controls the spatial extent of the basis set.[17,18,21] Typically, the scale factor is only applied to the most diffuse basis functions of the appropriate symmetry. A plot of the eigenvalues vs *z* displays avoided crossings that can be interpreted as resulting from the mixing of a relatively compact diabatic discrete state, the energy of which is only weakly dependent on the scale parameter, and DC solutions whose energies depend strongly on the scale parameter. A variety of methods have been introduced to extract resonance parameters from stabilization graphs.[16,48-51] Determination of the complex resonance energy can be accomplished by analytically continuing the energies as a function of *z* into the complex plane and locating complex

stationary points at which $\frac{dE}{dz} = 0$. This involves assuming a functional form for *E* in terms of *z* and fitting the data points on the stabilization graph to determine the parameters in this function. [16,49-51] Substitution of the appropriate stationary point into the expression for *E* gives the complex resonance energy. While one can employ data remote from the avoided crossing using Padé approximants for the analytic continuation,[52,53] in our applications we have focused on data points near an avoided crossing and have used generalized Padé approximants (GPAs),[16,54] which build in the branch point structure.

For isolated avoided crossings, involving two eigenvalues, the GPAs used in this work are of the form:

$$P(z)E^2 + Q(z)E + R(z) = 0 \tag{7}$$

where *P*, *Q*, and *R* are polynomials in *z* with the coefficients being determined by fitting two roots of a stabilization graph in the vicinity of an avoided crossing. The order of the GPA is specified by the order of the three polynomials, i.e., by (n_p, n_q, n_r). Based on prior studies,[55,56] we use $n_q = n_p + 1$ and $n_r = n_q + 2$, in which case the simplest GPA would be designated (0,1,2). In this work we used GPAs up to (4,5,6), using different sets of data points on two curves involved in an avoided crossing in least squares fitting of the coefficients in the three polynomials and averaging the results. When using high order GPAs, the AC procedure can lead to spurious stationary points. These are identified by their sensitivity to the choice of input points and are excluded from the averaging. For crossings involving three roots eqn (7) was extended to include terms that are cubic in *E.* In such cases the complex stationary energy converges with respect to the order of polynomial by the (5,6,7,8) GPA.

In the RAC procedure[22-24] an attractive term multiplied by a positive coupling constant λ is added to the potential. For sufficiently large values of λ the addition of this term converts the resonance into a bound state. To determine the resonance parameters, one expresses λ as a rational fraction fitting the coefficients in this expression to values of the momentum *k* for which the anion is bound. One then determines the *k* value at which λ = 0 to determine the complex resonance energy. we use the following equation from Barta and Horacek.[23]

$$\lambda(\kappa) = \lambda_0 \frac{(\kappa^2 + 2\alpha^2\kappa + \alpha^4 + \beta^2)(1 + \delta^2\kappa)}{\alpha^4 + \beta^2 + \kappa[2\alpha^2 + \delta^2(\alpha^4 + \beta^2)]} \tag{8}$$

where $\kappa = ik$, and α, β, and δ are parameters determined in the fitting procedure, and λ_0 is the value of λ for which the eigenvalue of interests changes from bound to unbound in the fit.

In the present application of the RAC method to the double well potentials considered here we add an attractive Gaussian of the form $-\lambda e^{-0.06r^2}$ at the origin. Calculations are carried out for λ values ranging from λ_0 to 3 with a step of 0.01. These results were used to determine optimal ranges of data points for the various RAC calculations which will be described below after the various basis sets used for the calculations are presented.

In the CAP method, an absorbing or negative imaginary potential –iηW is added to the Hamiltonian:

$$H_{CAP} = H - i\eta W \tag{9}$$

Here, η is a strength parameter, and *W* is normally a real potential that vanishes in the inner region, starts to grow at a cutoff radius r_0, and continues to grow with increasing distance from the system.[25,27] However, CAPs with complex *W* have been used.[57,58] Here we use a Voronoi CAP[59] with real *W*:

$$W = \begin{cases} 0, r_N \leq r_0 \\ (r_N - r_0)^2, r_N > r_0 \end{cases} \quad (10)$$

where r_N is the distance from the nearest site (1 or 2) and r_0 = 3 bohr (see eqn (4) in Ref. 58). Integrals of Voronoi CAPs must be evaluated numerically, and at every basis set site, a Lebedev-Teutler grid[60] with 770 angular and 199 radial points is used.

We note that in our CAP calculations the basis set is explicitly split into a core set and a DC-like set (details are provided below). CAP matrix elements involving core functions are set to zero; the CAP acts only on the DC-like basis functions of the respective basis sets. While the matrix elements affected by this procedure are very small, it helps to reinforce the idea that the CAP should only act in the asymptotic region so that the method is less dependent on the particular value of r_0.

In CAP calculations with complete basis sets, DC states appear as a discrete string that has been rotated into the fourth quadrant of the complex energy plane, and provided the Siegert energy has been uncovered by this rotation, it appears as an isolated eigenvalue. However, with finite basis sets, the picture is less tidy: For $\eta = 0$ all eigenvalues start on the real axis, and as η is increased all continuum eigenvalues migrate into the fourth quadrant. Resonances can be identified by the relatively small rate of change, $|\mathrm{d}E(\eta)/\mathrm{d} \ln \eta|$, of their complex trajectories, and the best representation of the resonance eigenvalue is found where this derivative of the resonance trajectory shows a minimum.[25,27,28] Resonance energies can be corrected for artificial reflections of the outgoing wave by the CAP[25], but unfortunately these corrections tend to enhance basis set errors, and here no correction was applied.

For the CAP calculations, the overlap matrix, the kinetic energy matrix, the integration grid, and the atomic-orbital to symmetry-orbital transformation matrices are supplied by the Python interface of Psi4 library functions, version 1.7.[61] The complex symmetric matrix representing the CAP Hamiltonian is then diagonalized using scientific Python (scipy).[62]

In the present study the bound state calculations are carried out with four different basis sets classes that differ slightly for the different bound state methods. All of the basis sets have, as a description of the molecular region, the first 10 even-tempered Gaussian functions used in the CKV calculations, with exponents ranging from 700 to 0.1835008 with successive exponents decreasing by a factor of 2.5. *I.e.*, the exponents are given by $700/(2.5)^n$, where n = 1 – 10. This set of basis functions is suitable for describing the bound Π state as well as the compact part of the resonance wavefunction. We thus refer to this set as core functions. As the core functions are the same for all basis sets, they will not be used as part of the basis set designations. The core basis is augmented either with diffuse *p* functions at each site, designated as (p + p), diffuse *p* functions located at the origin, designated as (P) or diffuse *d* functions located at the origin, designated as (D). The fourth basis set, designated as (p + p’), includes the same core functions at each site and the same diffuse *p* functions at the 1 site as the (p + p) basis set. However, in the (p + p’) basis set the exponents of the diffuse functions at site 2 are obtained by multiplying each of the diffuse exponents at site 1 by 1.25. This basis set introduces asymmetry in the diffuse basis functions, more realistically representing the situation in a heteronuclear diatomic in which the basis sets on the atoms would differ. While in the application of the stabilization method to a heteronuclear diatomic molecule the core basis functions associated with the two atoms would also differ, these were kept identical on the two sites to focus attention on the effect of asymmetry in the DC states due to the diffuse functions.

Table 2 summarizes the details of the construction of each basis set. The stabilization and RAC methods use the same basis sets. The (*p* + *p*) basis set for these methods is identical to the CKV basis set with five diffuse *p* on each site, continuing the progression in the set of core functions. The (p + p′) basis set also adds five diffuse *p* functions at each site with the asymmetry mentioned above. Ideally, only the additional diffuse functions in the (p + p) and (p + p′) basis sets would be scaled in the stabilization method. However, we have found it necessary to also scale the outermost most diffuse core function on each site in the stabilization calculations with these two basis sets. The need for this can be seen from consideration of potential set B for which the resonance interacts with the 7^{th} – 11^{th} DC states. Since only ten DC solutions are derived from the five diffuse functions on each site, in the stabilization calculations with the (p + p) and (p + p′) basis sets we also scale the most diffuse core function on each site. The (P) basis set has an even-tempered set of six *p* functions at the origin starting with an exponent of 0.5 and with consecutive exponents decreasing by a factor of 2.5. The (D) basis set is analogous to the (P) basis set except that the basis functions at the origin are *d* functions. We note that in the stabilization calculations with the (P) and (D) basis sets the exponents of the most diffuse core basis functions are not scaled.

Table 2. Basis set designations. [a,b]

(p + p)	(p + p′)	(P)	(D)
5p(1) + 5p(2)	5p(1) + 5p′(2)	6p[c]	6d[c]

[a] All basis sets include 10 core functions on each site as described in the text. Only the number and type of the supplemental diffuse functions are indicated.
[b] Listings reflect basis sets used in stabilization and RAC calculations while the number of functions are doubled for CAP calculations.
[c] Functions located at the origin.

For potentials B-F the RAC calculations with the (P), (p + p) (p + p′) basis sets used data points in the range of λ_0 to λ_0 + 0.35 in fitting eqn (8), while the calculations with the (D) basis set used data points in the range of λ_0 + 0.08 to λ_0 + 0.43 in fitting eqn (8). The latter choice of data points was also used for the symmetric potential A, for both the (D) and (p + p) basis sets. The choices of data points were established from a series of calculations using different starting points.

CAP calculations typically use smaller even-scaling factors in generating the diffuse basis set than stabilization calculations: Instead of exponent ratios of 2.5, ratios close to 1.5 are commonly used. Basis sets with more densely spaced diffuse functions are needed in CAP calculations because the basis must represent the oscillating wavefunction of the outgoing electron to the CAP cutoff r_0 and then for a certain distance in the CAP region until it has been absorbed.[63,64] Here, we use diffuse sets that match the diffuse exponent range of the stabilization basis sets, in other words, the first and last diffuse exponents are identical to those in the stabilization and RAC calculations. However, the number of even-tempered exponents in this range is increased until the exponent ratio is close to 1.5. Following this strategy, the (p + p) and (p + p′) basis sets consist of the core set augmented with 10 diffuse *p* functions at each site, while the (P) and (D) sets consist of the core set augmented with 12 exponents ranging from 0.5 to 0.005. All diffuse sets have exponent ratios of about 1.52.

To demonstrate the need for smaller even-scaling factors in CAP calculations, the convergence of the resonance energy is studied for the non-symmetric potential F and the (P) basis. Seven different (P) sets are constructed where the range of the exponents of the supplemental diffuse functions is unchanged (0.5 to 0.005), but the number of *p*-functions increases from six to 12 corresponding to an exponent ratio decrease from 2.5 to 1.52. The obtained resonance energies (Fig. 2) show a pattern of "spiraling" convergence in the complex plane in that the length of the complex step between subsequent resonance energies continuously decreases from 28meV (six to seven *p* functions) to finally 3meV (11 to 12 *p* functions) while at the same time the converged resonance energy is approached on a strongly curved complex trajectory. Based on this study, we expect the CAP basis set convergence to be significantly better than 10 meV.

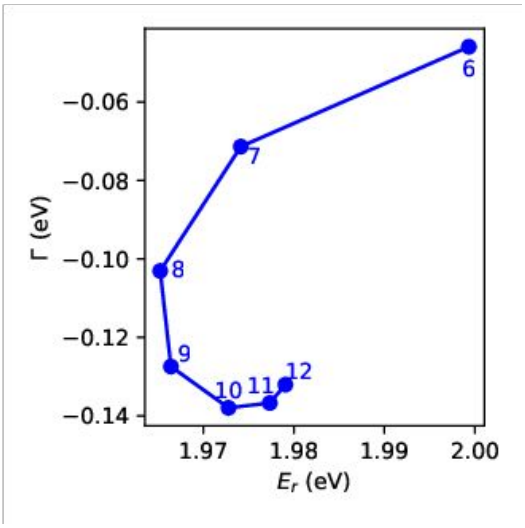

Fig. 2 Resonance energies of the potential defined by parameter set F computed with the CAP method and different (P) basis sets with six to 12 *p*-functions. With increasing number of basis functions, the exponent ratio drops from 2.5 (six functions) to about 1.8 (nine functions) and 1.52 (12 functions).

3 RESULTS AND DISCUSSION

In this section, we first discuss the change of the resonance parameters determined from the CKV calculations in going from the symmetric parameter set A to the most asymmetric set F. Then, we compare the CKV results with those obtained using bound state methods, investigate how the stabilization graphs depend on choice of basis set, and briefly consider the effect of asymmetric basis sets on the prediction of total widths.

3.1 Trends in Resonance Parameters with Change in Potential Parameters

Fig. 3 displays the total and partial widths obtained from CKV calculations as a function of E_r for each model potential considered. (The fitted parameters for each potential are reported in the ESI.) The resonance energy, E_r, decreases monotonically as the potential moves from symmetric (Set A, far right in the figure) to increasingly asymmetric, as expected since the asymmetry is produced in this model by deepening one of the wells. Additionally, the *p*-wave partial width monotonically increases from zero

for the symmetric potential while the *d*-wave partial width monotonically decreases with growing asymmetry in the potential. Interestingly, for asymmetric potentials sets B and C which have both *p*- and *d*-wave contributions, the leading partial wave does not have the larger partial width. Even for the most asymmetric potential considered (Set F), the *d*-wave partial width cannot be considered insignificant.

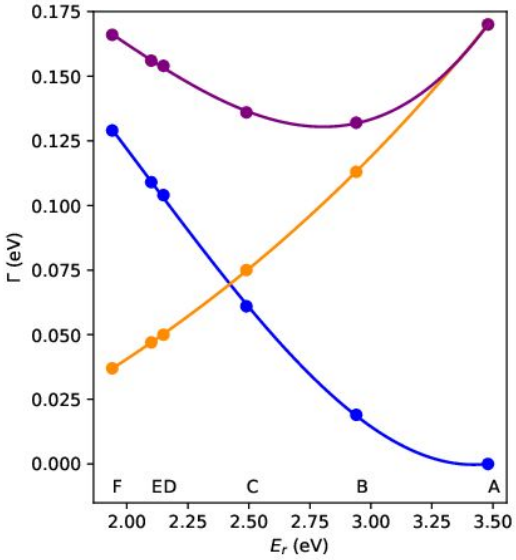

Fig. 3 Partial and total widths vs resonance position from the CKV method for all parameter sets A through F. The figure shows total (purple circles), *p* (blue circles), and *d* (orange circles) widths, with accompanying curves representing cubic fits to the respective data. The parameter set is indicated along the horizontal axis.

The trends in the partial widths track well with changes in shape of the orbital involved in electron capture as the potential becomes less symmetric. Fig. 4 shows the contour plots of orbitals obtained in the plateau or stabilized region of the stabilization graphs obtained with the (p + p) basis set for potential sets A, C, and F. The diminution of the orbital at the lower site in each figure, with accompanying augmentation at the other, in moving from set A to F corresponds with the change from a pure *d*-wave resonance for set A to a resonance dominated by *p*-wave scattering for set F. These trends are in line with intuitive expectations and show the sensitivity of the partial widths to the changes in the shape of the orbital involved in electron capture. Similar trends are observed in the stabilized CAP orbitals which are reported in the ESI.

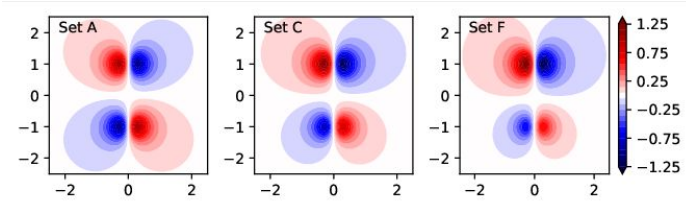

Fig. 4 Contour plot of the stabilized orbital obtained with the (p + p) basis set for potential sets A (left), C (middle) and F (right). A cut through the yz axis is shown. (As the resonance is a degenerate π orbital, the xz and yz cuts of respective π components are identical.) All panels show the same range. The units on the horizontal (z) and vertical (y) axes are bohr. The value of the orbital is indicated by the color scale on the right, which has units of $(\text{bohr})^{-3/2}$.

3.2 Resonance Positions, Partial and Total Widths from the Various Methods

Fig. 5 highlights the deviations of the partial widths predicted by each bound state method from the corresponding value obtained from the CKV calculations. (The complete set of resonance parameters obtained from each method is contained in the ESI.) The partial widths from the stabilization and CAP methods are in good agreement with the CKV results (with the deviations being 10% or less, and typically less than 5%) while those for the RAC method can be significantly greater (typically less than 20%). Most importantly, all three bound state methods capture the essential trends in the absolute as well as relative magnitudes of the partial widths.

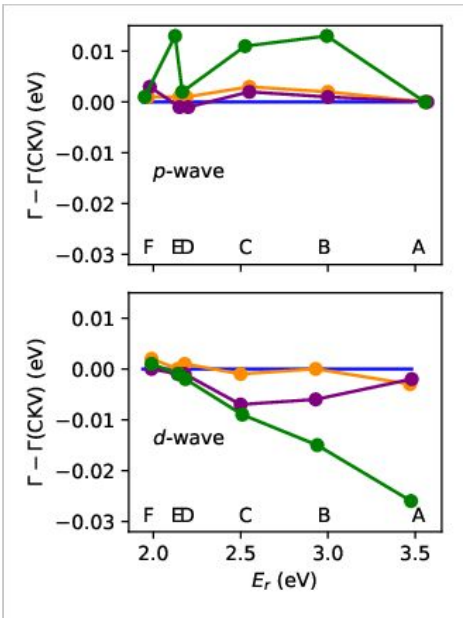

Fig. 5 Deviation (in eV) of the partial widths from the bound state calculations from the CKV results. *p* (top) and *d* (bottom) partial widths. CAP (purple circles). stabilization (orange circles) and RAC (green circles) methods, with the accompanying lines simply connecting the dots to aid the eye. The parameter set is indicated along the horizontal axis.

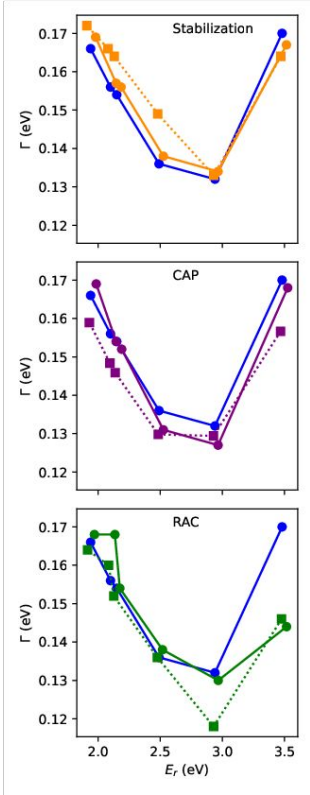

Fig. 6 Comparison of total widths as function of resonance positions from the bound state methods to the CKV results. The three panels show resonance width vs position for the six parameter sets A to F. From the top, the panels compare stabilization (orange), CAP (purple), and RAC (green) results with the CKV (blue) method. For the bound state methods both the total width obtained with the (p + p) basis (circles connected with solid line) and the total width obtained as sum of the *p* and *d* partial widths (squares connected with dotted line) are shown. The parameter set is indicated along the horizontal axis.

Two approaches to obtaining the total resonance width for each bound state method were considered. The first approach was to take the total width to be the sum of the partial widths, which is expected to be a good approximation for the relatively narrow resonances considered here. This was also the approach used to obtain the total width for the CKV calculations. In addition, the bound state calculations using the (p + p) basis set provide a direct estimate of the total width. The E set of results is contained in the ESI. Fig. 6 summarizes the results by displaying in each panel the CKV total width (from the sum of the partial widths), the sum of the partial widths for the given bound state method, and the bound state results obtained using the (p + p) basis set.

There is semi-quantitative agreement between the total widths from the various bound state methods and the CKV results. For the stabilization calculations the total widths from the sum of the partial widths agrees better with the CKV results than the total widths obtained using the (p + p) basis set. The difference between the sum and the (p + p) basis set results is not as pronounced for the CAP results. For the RAC calculations the agreement is markedly worse for sets A and B.

3.3 Qualitative analysis of stabilization graphs obtained with different basis sets

Fig. 7, presents stabilization graphs obtained using the (P), (D), (p + p) and (p + p') basis sets for potential set C. Except for set A, for which the (P) basis set gives a zero partial width, these stabilization graphs are representative of those found for all potentials considered in this study. For both the (P) and (D) basis sets, examination of the DC orbitals indicate that they can be approximated as possessing well defined angular momentum. In each case, the stabilization graphs for the (P) and (D) basis sets therefore show simple two-state avoided crossings that describe the coupling of the resonance to the respective continuum, and analytic continuation provides the partial width for the appropriate partial wave.

In contrast, for the (p + p) basis set, three states are involved in the avoided crossing in the case of the asymmetric potentials. Examination of the wavefunctions of the DC solutions that interact with the discrete state confirm that one is dominantly *p*-wave while the other is predominantly *d*-wave. A cubic GPA is used to fit the energies of the three interacting levels (i.e., the discrete state and the *p* and *d* partial wave DC solutions). Analytic continuation provides an approximation to the total width as seen from Fig. 6.

The stabilization graph for the (p + p') basis set differs appreciably from that obtained with the (p + p) basis set. Rather than having three strongly interacting roots over a small range of scale parameters, the latter stabilization graph has a series of well isolated two root avoided crossings which alternate between narrow and broad. Examination of the DC orbitals shows that for this basis set each DC level is a strong admixture of *p* and *d* waves. As expected from the different shapes of the avoided crossings, a range of widths is obtained from analytic continuation using different ranges of input data, as discussed in the next section.

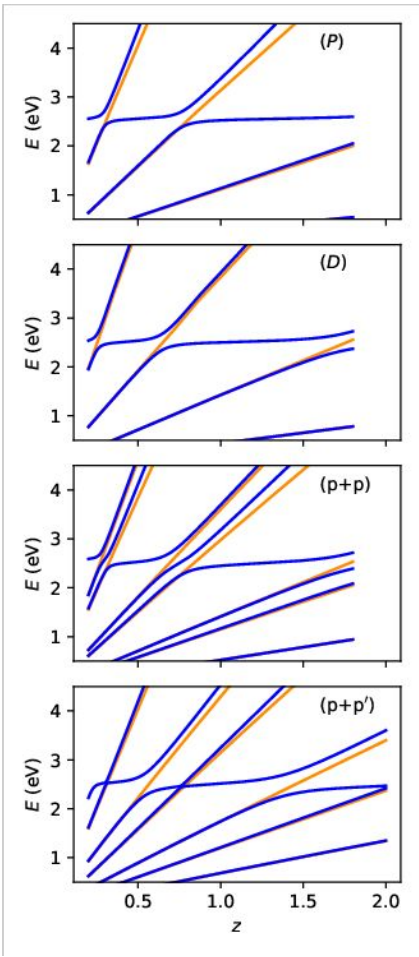

Fig. 7 Stabilization graph for parameter set C showing the eigenvalues (in eV), as a function of the scale parameter (*z*), of the two-site model (blue) and the DC energies (orange), both in eV, obtained with: (P), (D), (p + p) and (p + p′) basis sets in panels a, b, c, and d, respectively.

3.4 Effect of Asymmetric Basis Sets on the Prediction of Total Widths

The (p + p′) basis set was designed to incorporate the asymmetry typically found in basis sets used in heteronuclear diatomic molecules. For the CAP and RAC methods there is little difference between the total widths predicted with the (p + p) and (p + p′) basis sets. However, analytic continuation applied to the isolated crossings in stabilization graph using the (p + p′) basis set depicted in Fig. 7d provides widths that are neither total nor partial widths. For the data presented in Fig. 7d the following widths are found for the five crossings from left to right in the figure: 0.016, 0.129, 0.020, 0.135 and 0.022 eV. Recall that widths obtained from stabilization calculations using the (P), (D), and (p + p) basis sets were 0.064 eV, 0.074 eV, 0.149 eV, respectively. With the (p + p′) basis set the DC levels and the orthogonalized DC (ODC) levels, the latter of which includes orthogonalization to the discrete state (and to the bound state), alternate between being localized around one potential well or the other. Since the discrete state is localized in the vicinity of the potential well at r_1, this results in alternating narrow

and broad avoided crossings in the stabilization graph. The coupling between the wavefunction of the discrete state and that of the ODC level is small when the latter is localized in the well centered at r_1 and larger when it is localized around the well centered at r_2 due to the extra lobes in the wave functions of the ODC levels. These results indicate that widths derived from stabilization calculations using traditional basis sets for molecular calculations need to be carefully checked to determine whether they correspond to partial or total widths, or to neither (i.e., to some ill-defined combination of the partial widths).

4 Conclusions

In this work we consider a series of double-well potentials that support a low-lying shape resonance analogous to the π^* temporary anions of N_2 and CO. For the symmetric potential the resonance is of Π_g symmetry, and is *d*-wave in character, while for the asymmetric potentials the resonance has both *p*-wave and *d*-wave contributions, with the relative weights of these components depending on the degree of asymmetry in the potential. The complex Kohn variational method is used to determine the positions and partial widths of the resonance, via fitting the *T*-matrix elements as a function of energy to functional forms based on the work of Blatt and Weisskopf.[47] These serve as a basis for assessing the performance of the stabilization, regularized analytic continuation, and the complex absorbing potential methods for obtaining the partial and total widths. It is found that all three bound state methods, when employed with appropriate basis sets, give partial widths in good agreement with the CKV results, with the agreement being better for the stabilization and CAP methods than for the RAC method. Each method also provides good estimates of the total widths either by summing the partial widths or by extracting the total width directly from calculations using a basis set containing diffuse basis functions on each site. We also demonstrate that with certain basis sets, the stabilization method can give widths that do not correspond closely to either a partial width or a total width. However, the use of single center expansion for the diffuse functions not only allows the determination of partial widths but also simplifies the analysis of the stabilization graphs. The ability of all three bound state methods to predict partial widths confirms the approach used in Ref. 18 to calculate complex potential energy surfaces that include partial widths over a range of geometries, allowing calculations of differential cross sections for elastic and inelastic scattering. While the partial widths rigorously sum to the total width only in the limit of narrow resonances, the success of this approach in predicting the absolute magnitude, energy dependence and angular dependence of the vibrational excitation of CO via the $^2\Pi$ resonance in Ref. 18, suggests that this approximation serves well enough for at least moderately broad resonances within experimental resolution.

We note also that the approach presented here provides a solution to a major problem in applying the stabilization method to polyatomic molecules such as butadiene and anthracene for which different avoided crossings can give very different widths. This problem is caused by the fact that the DC levels involved in the various avoided crossings have different weights on the relevant partial waves. By using single center expansions of diffuse functions in specific angular momenta one can obtain well defined partial widths that can be summed to give the total widths.

Conflicts of Interest: There are no conflicts of interest to declare.

Acknowledgments: T.S. gratefully acknowledges support from the National Science Foundation under Grant No. 2303652. S.S. acknowledges support from a Mellon Fellowship from the University of Pittsburgh. We thank W. C. McCurdy for helpful discussions concerning the complex Kohn variational

procedure. We also thank J. Nichols for work on the complex Kohn code while he was supported by a Swezey Summer Research grant from Gove City College.

References

1. G. Schulz, Resonances in Electron Impact on Diatomic Molecules*, Rev. Mod. Phys.,* 1973, **45**, 423–486.

2. K. D. Jordan and P. D. Burrow, Temporary Anion States of Polyatomic Hydrocarbons, *Chem. Rev.,* 1987, **87**, 557–588.

3. J. Simons, Molecular Anions, *J. Phys, Chem. A*, 2008, **112**, 6401–6511.

4. J. Simons, Molecular Anions Perspective, *J. Phys. Chem. A*, 2023, **127**, 3940–3957.

5. M. Ranković, P. Nag, C.S. Anstöter, G. Mensa-Bonsu, T. P. Kumar, J. R. Verlet and J. Fedor, Resonances in Nitrobenzene Probed by the Electron Attachment to Neutral and by the Photodetachment from Anion, *J. Chem Phys.,* 2022, **157**, 064302.

6. Z. Li, Y. Zheng, P. Cloutier, L. Sanche and J.R. Wagner*,* Low Energy Electron Induced DNA Damage: Effects of Terminal Phosphate and Base Moieties on the Distribution of Damage *J. Am. Chem. Soc.*, 2008, **130**, 5612–5613.

7. X. Wang, H. Liao, W. Liu, Y. Shao, Y. Zheng and L. Sanche, DNA Protection against Damages Induced by Low-Energy Electrons: Absolute Cross Sections for Arginine–DNA Complexes, *J. Phys. Chem. Lett.*, 2023, **14**, 5674–5680.

8. G. A. Cooper, C. J. Clark and J. R. Verlet, Low-Energy Shape Resonances of a Nucleobase in Water*, J. Am. Chem. Soc.*, 2023, **145**, 1319 –1326.

9. D. C. Tyte, Carbon Dioxide Lasers*, Advances in Quantum Electronics,* 1970, **1**.

10. T. N. Rescigno, C. W. McCurdy, A. E. Orel and B. H. Lengsfield, The Complex Kohn Variational Method, *Computational Methods for Electron—Molecule Collisions,* 1995, 1–44.

11. B. Schneider, R-Matrix Theory for Electron-Atom and Electron-Molecule Collisions Using Analytic Basis Set Expansions, *Chem. Phys. Lett.,* 1975, **31**, 237–241.

12. C. W. McCurdy and T. N. Rescigno, Collisions of Electrons with Polyatomic Molecules: Electron-Methane Scattering by the Complex Kohn Variational Method*, Phys. Rev. A,* 1989, ***39***, 4487–4493.

13. R. F. Da Costa, M. T. Varella, M. H. Bettega and M. A. Lima, Recent Advances in the Application of the Schwinger Multichannel Method with Pseudopotentials to Electron-Molecule Collisions*, Euro. Phys. J. D*, 2015, **69**, 1–24.

14. H. Su, X. Cheng, B. Cooper, J. Tennyson and H. Zhang, Electron-Impact High-Lying N_2^- Resonant States, *Phys. Rev. A,* 2022, ***105***, 062824.

15. A. U. Hazi and H. S. Taylor, Stabilization Method of Calculating Resonance Energies: Model Problem*, Phys. Rev. A*, 1970, **1**, 1109–1120.

16. J. S. Chao, M. F. Falcetta and K. D. Jordan, Application of the Stabilization Method to the N_2^- ($1\ ^2\Pi_g$) and Mg^-($1\ ^2P$) Temporary Anion States, *J. Chem Phys.*, 1990, **93**, 1125–1135.

17. M. F. Falcetta, L. A. DiFalco, D. S. Ackerman, J. C. Barlow and K.D. Jordan, Assessment of Various Electronic Structure Methods for Characterizing Temporary Anion States: Application to the Ground State Anions of N_2, C_2H_2, C_2H_4, and C_6H_6, *J. Phys. Chem. A*, 2014, **118**, 7489–7497.

18. M. F. Falcetta, M. C. Fair, E. M. Tharnish, L. M. Williams, N. Hayes and K. D. Jordan, *Ab Initio* Calculation of Electron Impact Vibrational Excitation of CO via the $^2\Pi$ Shape Resonance*, J. Chem. Phys.,* 2016, **144***,* 104303:1–8.

19. N. Moiseyev, Quantum Theory of Resonances: Calculating Energies, Widths and Cross-Sections by Complex Scaling, *Phys Rep*, 1998, **302**, 212–293.

20. M. Thodika and M. Fennimore and T. N. V. Karsili and S. Matsika, Comparative Study of Methodologies for Calculating Metastable States of Small to Medium-Sized Molecules, *J. Chem. Phys.*, 2019, **151**, 244104.

21. M. A. Fennimore and S. Matsika, Electronic Resonances of Nucleobases using Stabilization Methods, *J. Phys. Chem. A*, 2018, **122**, 4048-4057.

22. A. F. White, M. Head-Gordon and C. W. McCurdy, Stabilizing Potentials in Bound State Analytic Continuation Methods for Electronic Resonances in Polyatomic Molecules, *J. Chem. Phys.*, 2017, ***146***, 44112.

23. T. Bárta and J. Horáček, Calculation of Resonances by Analytical Continuation: Role of Asymptotic Behavior of Coupling Function*, Phys. Scr.*, 2020, ***95***, 065401–065409

24. J. Horáček, I. Paidarová and R. Čurík, On a Simple Way to Calculate Electronic Resonances for Polyatomic Molecules, J. *Chem. Phys.*, 2015, **143**, 184102.

25. U. V. Riss and H. D. Meyer, Calculation of Resonance Energies and Widths Using the Complex Absorbing Potential Method, *J. Phys. B: At. Mol. Opt. Phys., 1993*, **26**, 4503–4535.

26. T. C. Jagua and K. B. Bravaya, A. I. Krylov, Extending Quantum Chemistry of Bound States to Electronic Resonances, *Ann. Rev. of Phys. Chem*., 2017, ***68***, 525–553.

27. R. Santra and L. S. Cederbaum, Non-Hermitian electronic theory and applications to clusters*, Phys. Rep.* 2002, **368**, 1–117.

28. J. U. Davis and T. Sommerfeld, Computing resonance energies directly: method comparison for a model potential*, Eur. Phys. J. D.*, 2021, **75***,* 316:1–12.

29. T. Sommerfeld, U. V. Riss, H. D. Meyer, L. S. Cederbaum, B. Engels and H.U. Suter, Temporary Anions - Calculation of Energy and Lifetime by Absorbing Potentials: The Resonance, *J. Phys. B: At. Mol. Opt. Phys.*, 1998, **31**, 4107–4122.

30. D. Zuev, T. C. Jagua, K. B. Bravaya, E. Epifanovsky, Y. Shao, E. Sundstrom, M. Head-Gordon and A. I. Krylov, Complex Absorbing Potentials within EOM-CC Family of Methods: Theory, Implementation, and Benchmarks*, J. Chem. Phys.*, 2014, **141**, 24102.

31. A. F. White, M. Head-Gordon and C.W. McCurdy, Complex Basis Functions Revisited: Implementation with Applications to Carbon Tetrafluoride and Aromatic N-Containing Heterocycles within the Static-Exchange Approximation, *J. Chem. Phys.*, 2015, **142**, 54103.

32. T. N. Rescigno, A. E. Orel and C. W. McCurdy, Application of Complex Coordinate SCF Techniques to a Molecular Shape Resonance: The $^2\Pi_g$ State of N_2^-, *J. Chem. Phys.*, 1980, **73**, 6347–6348.

33. I. Jana, S. Basumallick, S. Paland and N. Vaval, Effect of Partial Triples Excitation Using Complex Absorbing Potential-Based Fock-Space Multi-Reference Coupled Cluster*, Int. J. Quant. Chem.*, 2021, **121**, e26738.

34. M. Banuary and A. K. Gupta, Application of Modified Smooth Exterior Scaling Method to Study $^2\Pi_g$ N_2^- and $^2\Pi$ CO^- Shape Resonances, *ACS Omega*, 2023, **8**, 7143–7150.

35. A. J. Seigert, On the Derivation of the Dispersion Formula for Nuclear Reactions, *Phys. Rev*., 1939, **56**, 750–752.

36. M. Allan, Measurement of Absolute Cross Sections of Electron Scattering by Isolated Molecules, in Low-Energy Electron Scattering from Molecules, Biomolecules and Surfaces*, Carsky, P.; Curik, R. eds. CRC Press* 2012, 43–90.

37. S. R. Slimak, M. F. Falcetta and K. D. Jordan, unpublished results.

38. T. F. O'Malley and H. S. Taylor, Angular Dependence of Scattering Products in Electron-Molecule Resonant Excitation and in Dissociative Attachment*, Phys. Rev.*, 1968, **176**, 207–221.

39. H. Ehrhardt, L. Langhans, F. Linder and H.S. Taylor, Resonance Scattering of Slow Electrons from H_2 and CO Angular Distributions, *Phys. Rev.*, 1968, **173**, 222–230.

40. E. S. Chang, Theory of Angular Distributions of Electrons Resonantly Scattered by Molecules. I. Vibrational and Rotational Excitation of Diatomic Molecules, *Phys. Rev. A.*, 1977, **16**, 1841–1849.

41. E.S. Chang, Theory of Angular Distributions of Electrons Resonantly Scattered by Molecules. II. Vibrational and Rotational Excitation of CO*, Phys. Rev. A.*, 1977, **16**, 1850–1853.

42. F. H. Read, Angular Distributions for Resonant Scattering of Electrons by Molecules, *J. Phys. B: At. Mol. Phys.*, 1968, **1**, 893–908.

43. D. K. Watson, Partial Widths and Resonance Normalization, *Phys. Rev. A.*, 1986, **34**, 1016–1025.

44. J. Bentley and D. M. Chipman, Partial Widths of Resonances by Analytic Continuation from Real Eigenvalues, *Chem. Phys. Lett.*, 1990, **167**, 246–251.

45. J. R. Taylor, Scattering Theory: The Quantum Theory of Nonrelativistic Collisions; *Robert F. Krieger Publishing,* 1983.

46. U. Fano, Effects of Configuration Interaction on Intensities and Phase Shifts*, Phys. Rev.*, 1961, **124**, 1866-1878.

47. J. M. Blatt and V. F. Weisskopf, Theoretical Nuclear Physics; *John Wiley & Sons, Inc.*, 1952.

48. J. Simons, Resonance State Lifetimes from Stabilization Graphs, J. *Chem. Phys.*, 1981, **75**, 2465–2467.

49. J. Simons, Analysis of Stabilization and Extrapolation Methods for Determining Energies and Lifetimes of Metastable Electronic States, *J. Phys. Chem. A*, 2021, **125**, 7735–7749.

50. A. D. Isaacson and D. G. Truhlar, Real-Basis-Function Method with Correct Branch-Point Structure for Complex Resonances Energies, *Chem. Phys. Lett.*, 1984, **110**, 130–134.

51. C. W. McCurdy and J. F. McNutt, On the Possibility of Analytically Continuing Stabilization Graphs to Determine Resonance Positions and Widths Accurately, *Chem. Phys. Lett.,* 1983, ***94***, 306–310.

52. A. Landau, I. Haritan, P. R. Kaprálová-Ždánská and and N. Moiseyev, Atomic and Molecular Complex Resonances from Real Eigenvalues Using Standard (Hermitian) Electronic Structure Calculations, *J. Phys. Chem. A*, 2016, **120**, 3098–3108.

53. A. Landau and I. Haritan, A Systematic Search for the Resonance Energies Obtained via Padé, J. *Phys. Chem. A*., 2019, **123**, 5091–5105.

54. K. D. Jordan, Construction of Potential Energy Curves in Avoided Crossing Situations, *Chem. Phys.*, 1975, **9**, 199–204.

55. B. J. Carlson, M. F. Falcetta, S. R. Slimak and K. D. Jordan, A Fresh Look at the Role of the Coupling of a Discrete State with a Pseudocontinuum State in the Stabilization Method for Characterizing Metastable States, *J. Phys. Chem. Lett.*, 2021, **12**, 1202–1206.

56. S. R. Slimak, K. D. Jordan and M.F. Falcetta, Role of Overlap between the Discrete State and Pseudocontinuum States in Stabilization Calculations of Metastable States, *J. Phys. Chem. A*, 2021, **125**, 4401–4408.

57. D. E. Manolopoulos, Derivation and Reflection Properties of a Transmission-Free Absorbing Potential*, J. Chem. Phys.*, 2002, **117**, 9552–9559.

58. Y. Sajeev, V. Vysotskiy, L. S. Cederbaum and N. Moiseyev, Continuum Remover-Complex Absorbing Potential: Efficient Removal of the Nonphysical Stabilization Points, *J. Chem. Phys.*, 2009, **131**, 211102.

59. T. Sommerfeld and M. Ehara, Complex Absorbing Potentials with Voronoi Isosurfaces Wrapping Perfectly around Molecules, *J. Chem. Theory Comput.*, 2015, **11**, 4627–4633.

60. V. I. Lebedev and D. N. Laikov, A Quadrature Formula for the Sphere of the 131st Algebraic Order of Accuracy*, Dokl. Math*, 1999, **59**, 477–481.

61. D. G. Smith, L. A. Burns, A. C. Simmonett, R. M. Parrish, M.C. Scheiber, R. Galvelis, P. Kraus, H. Kruse, R. Di Remigio, A. Alenaizan, A.M. James, S. Lehtola, J. P. Misiewicz, M. Scheurer, R. A Shaw, J. B. Schriber, Y. Xie, Z. L. Glick, D. A. Sirianni, J .S. O'Brien, J. M. Waldrop, A. Kumar, E. G. Hohenstein, B. P. Pritchard, B. R. Brooks, H. F. Schaefer, A. Y. Sokolov, K. Patkowski, A. E. Deprince, U. Bozkaya, R. A. King, F. A. Evangelista, J. M. Turney, T. D. Crawford and C. .D. Sherrill, P SI4 1.4: Open-Source Software for High-Throughput Quantum Chemistry, *J. Chem. Phys.*, 2020, **152**, 184108.

62. P. Virtanen, R. Gommers, T. E. Oliphant, M. Haberland, T. Reddy, D. Cournapeau, E. Burovski, P. Peterson, W. Weckesser, J. Bright, S. J. van der Walt, J. Wilson, K. J. Millman, N. Mayorov, A. R. Nelson, E. Jones, R. Kern, E. Larson, C. J. Carey, İ. Polat, Y. Feng, E. W. Moore, J. VanderPlas, D. Laxalde, J. Perktold, R. Cimrman, I. Henriksen, E. A. Quintero, C. R. Harris, A. M. Archibald, A. H. Ribeiro, F. Pedregosa, P. van Mulbregt, A. Vijaykumar, A. P. Bardelli, A. Rothberg, A. Hilboll, A. Kloeckner, A. Scopatz, A. Lee, A. Rokem, C. N. Woods, C. Fulton, C. Mason, C. Häggström, C. Fitzgerald, D. A. Nicholson, D. R. Hagen, D. V. Pasechnik, E. Olivetti, E. Martin, E. Wieser, F. Silva, F. Lenders, F. Wilhelm, G. Young, G. A. Price, G. L. Ingold, G. E. Allen, G. R. Lee, H. Audren, I. Probst, J. P. Dietrich, J. Silterra, J. T. Webber, J. Slavič, J. Nothman, J. Buchner, J. Kulick, J. L. Schönberger, J. V. de Miranda Cardoso, J. Reimer, J. Harrington, J. L. Rodríguez, J. Nunez-Iglesias, J. Kuczynski, K. Tritz, M. Thoma, M. Newville, M. Kümmerer, M. Bolingbroke, M. Tartre, M. Pak, N. J. Smith, N. Nowaczyk, N. Shebanov, O. Pavlyk, P. A. Brodtkorb, P. Lee, R. T. McGibbon, R. Feldbauer, S. Lewis, S. Tygier, S. Sievert, S. Vigna, S. Peterson, S. More, T. Pudlik, T. Oshima, T. V. Pingel, T. P. Robitaille, T. Spura, T. R. Jones, T. Cera, T. Leslie, T. Zito, T. Krauss, U. Upadhyay, Y.

O. Halchenko, Y. Vázquez-Baeza, SciPy 1.0: Fundamental Algorithms for Scientific Computing in Python, *Nat Methods* 2020, **17**, 261–272.

63. U. V Riss and H. D. Meyer, Investigation on the Reflection and Transmission Properties of Complex Absorbing Potentials, *J. Chem. Phys.* 1996, **105**, 1409–1419.

64. K. Kaufmann, W. Baumeister and M. Jungen, Universal Gaussian Basis Sets for an Optimum Representation of Rydberg and Continuum Wavefunctions*, J. Phys. B: At. Mol. Opt. Phys.*, 1989, **22**, 2223–2240.